Journal of Molecular Liquids 435 (2025) 128147

Contents lists available at ScienceDirect

Journal of Molecular Liquids

journal homepage: www.elsevier.com/locate/molliq

The role of hydrogen bond formation in the extracting efficiency of NADES formulations

Dries Bleus [a], Renaud B. Jolivet [b], Wouter Marchal [a], Dries Vandamme [a,*,1], Katarzyna Dziubinska-Kuehn [b,*,1]

[a] Hasselt University, Campus Diepenbeek Gebouw D, Diepenbeek, 3590, Belgium
[b] Maastricht University, Paul-Henri Spaaklaan 1, Maastricht, 6229 EN, Netherlands

ARTICLE INFO

Keywords:
Extraction media
NADES
Nuclear magnetic resonance
Hydrogen bonding

ABSTRACT

The simplicity and versatility of natural deep eutectic solvents (NADES), together with a wide range of potential applications, make them great candidates to fight the lack of sustainability and circularity in large-scale industrial chemistry. Among the most prominent applications of NADES, extraction of phenolic compounds (PC) from natural sources remains one of the most attractive ones, due to the high commercial value of both, solvent and solute. In the present study, an in-depth analysis of the underlying mechanisms of extraction in NADES-PC systems is performed via quantification of the spin-spin interactions using 2D NMR experiments. The structure of the hydrogen bond donor, acceptor-to-donor molecular ratio, or number and distribution of the hydroxyl groups are determined as key components governing the solubility of PC in NADES. Moreover, our results reveal how studying the solvent hydrogen bond network formation between the NADES acceptor and donors can be easily translatable into understanding the solvation patterns and predicting the solubility efficiency of PC at low concentrations, below the level of direct detection.

1. Introduction

Non-aqueous solvents, such as ionic liquids (IL) and deep eutectic solvents (DES), have quickly become irreplaceable in biotechnology research and development, serving as alternatives to organic reaction, biocatalysis, or separation media [1,2]. Their possible application areas are currently expanding to the use of natural deep eutectic solvents (NADES) for the extraction of bioactive compounds [3,4] or greenhouse gases [5]. NADES are particularly efficient for this due to their high biocompatibility, dissolution capacity, selectivity, and stability [6].

The attractive properties of NADES originate from the characteristic two- or three-component formulations, where the hydrogen bond acceptor (HBA) and donor (HBD) molecules form an extensive hydrogen bond (HB) network [7,8]. Due to a high number of possible HBA (e.g. quaternary ammonium salts or metal halides) and HBD (e.g. polyols, carboxylic acids, or sugars) combinations, the physicochemical properties of DES can be precisely tailored to specific applications, hence their frequent description as designer solvents [9]. Furthermore, NADES are formed in one-pot synthesis, using non-toxic substrates of natural origin, such as plant-based metabolic products [10,11].

In recent years, the adaptability of NADES for extraction applications was confirmed in several studies [12,13]. These works were driven by a similar motivation: to obtain the highest extraction yield for selected solvent-solute combinations [14]. The efficiency of the extraction process is highly dependent on the pair of compounds investigated and on its conditions. This dependency is frequently attributed to the specific physicochemical properties of the DES, such as the mass transport limitations due to the inherent viscosity, or solute molecule(s) [15,16]. Thus, it remains difficult to generalize the trends given the high number of possible HBA, HBD, and solute combinations or the wide diversity of applied extraction conditions available in the literature.

The application of NADES as extraction media needs to be evaluated on a case-to-case basis. The current state-of-the-art mainly comprises empirical work, where solvents, matrices, and targeted extracts are systematically tested with different experimental protocols. For example, Ozturk and colleagues reported a high dependence of the yields

* Corresponding authors.
E-mail addresses: dries.vandamme@uhasselt.be (D. Vandamme), k.dziubinska@kbfi.ee (K. Dziubinska-Kuehn).
[1] Current address: National Institute of Chemical Physics and Biophysics, Akadeemia tee 23, 12618 Tallinn, Estonia.

https://doi.org/10.1016/j.molliq.2025.128147
Received 4 April 2025; Received in revised form 7 July 2025; Accepted 11 July 2025
Available online 16 July 2025

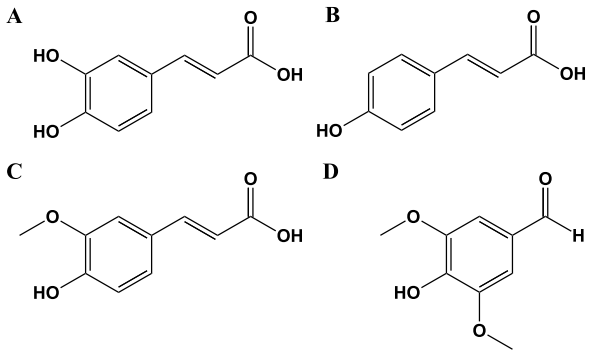

Fig. 1. Structures of four phenolic compounds used in the study: **A:** caffeic acid (CAF); **B:** *p*-coumaric acid (COU); **C:** ferulic acid (FER); **D:** syringaldehyde (SYR).

on the structure of HBD [17]. The most efficient extraction of common (poly)phenolic compounds (PC) from the orange peel was obtained while using NADES consisting of choline chloride (ChCl) and polyols, such as glycerol (Gly) or ethylene glycol (EG). In our previous work, we tested glyceline and malicine to extract four types of PC from Brewer's spent grain and malt dust [18]. Similar observations were made in [19] and [20]. Therein, ChCl:Gly NADES was used in the microwave-assisted extraction of PC from Brewer's spent grain and olive pomace. Studies by De Almeida Pontes, Zannou, and colleagues demonstrated the high hydrogen-bonding capability of ChCl-based NADES as a basis for strong solvent-solute interactions [21–23]. The addition of water was shown to modify solvent polarity, while the simultaneous presence of acidic HBD increased extraction efficiency.

PC are defined as a class of aromatics with one or more hydroxyl (OH) groups bound directly to the aromatic ring [24]. They are often responsible for structural and protective functions in plants, and can be extracted to serve as natural bioactive compounds [23,25]. Furthermore, their chemical structure is commonly linked to interesting biological properties, such as antioxidative, anti-inflammatory, and antimicrobial activity, and typically originates from the ability of PC molecules to react with free radicals [26]. Outside of medicine, PC have also found applications in the food and textile industries [27,28].

In the present work, we systematically analyze the impact of the PC on the NADES HB network using advanced nuclear magnetic resonance (NMR) methodology. Two NADES with different HBD and HBA:HBD ratios (1:2 ChCl:Gly and 1:1 ChCl:MA (malic acid)) were paired with four exemplary PC, including three hydroxycinnamic acids (caffeic acid, CAF (**A** in Fig. 1); *p*-coumaric acid, COU (**B**); ferulic acid, FER (**C**)) and a phenolic aldehyde, (syringaldehyde, SYR (**D**)) to assess whether high extraction yields can be explained by changes in the NADES-extract HB formation, or by NADES HB rearrangements. Understanding the intra- and intermolecular solvent-solute interactions is emphasized because it remains one of the crucial steps to accelerate sustainable developments in industrial chemistry.

2. Materials and methods

2.1. Materials

The natural deep eutectic solvents substrates DL-malic acid (≥99% purity, MA), glycerol (≥99%, Gly) and choline chloride (99%, ChCl) were purchased from Thermo Fischer Scientific (Waltham, USA). Caffeic acid (≥99%, CAF), *p*-coumaric acid (≥99%, COU), and ferulic acid (≥98%, FER) were purchased from Thermo Fischer Scientific (Waltham, USA). Syringaldehyde (≥98%, SYR) was purchased from TCI Chemicals (Tokyo, Japan). All chemicals were dried under vacuum at 60°C for 48 h prior to sample preparation. After purification, they were transported to a glovebox under N_2 atmosphere, where the NADES were synthesized and NMR samples were prepared. Samples containing water were prepared outside of the glovebox.

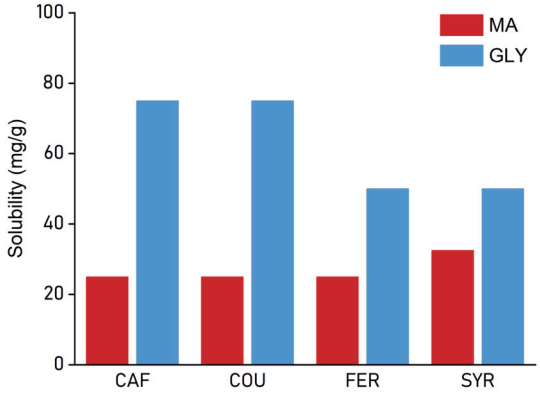

Fig. 2. Solubility of phenolic compounds (PC) in 1:1 ChCl:MA (malicine, red) and 1:2 ChCl:Gly (glyceline, blue) natural deep eutectic solvents (NADES), The bar chart shows the solubility expressed as miligram of PC per gram of NADES (mg/g). **CAF:** caffeic acid; **COU:** *p*-coumaric acid; **FER:** ferulic acid; **SYR:** syringaldehyde.

2.2. NADES synthesis

NADES were synthesized using the heat and stir method (for details, see [18]). MA and ChCl were mixed with a 1:1 molar ratio to form malicine. Gly and ChCl were mixed at 2:1 molar ratio to form glyceline. Substrates were weighed, combined, and stirred using a magnetic stirrer at 70°C for 3-5 h, under N_2 atmosphere. The NADES were left to cool down and rest at 25°C to allow the complete dissolution of solid components and dissipation of air bubbles formed during synthesis.

2.3. Mixtures of NADES and phenolic compounds

All mixtures were prepared in 5 mL glass vials, dried at 105°C, and brought to room temperature (RT) in a desiccator. Dried phenolic compounds were weighed directly in the glass vials with 0.01 mg precision. Next, 2.0 g of NADES was added to each PC under N_2 atmosphere with a maximum weight deviation of 1%, the vials were capped and transferred to the glovebox. The mixtures were stirred at 70°C for at least 24 h until the phenolic compounds were fully dissolved. Finally, they were cooled down at RT for 12 h, before further manipulations.

All samples were analyzed using high-pressure liquid chromatography (HPLC), and phenolic content was determined based on the external calibration curve, following the protocol in [18]. All solutions prepared using malicine, glyceline, and four phenolic compounds (CAF, COU, FER and SYR) are presented in Table S1. In addition, the ^{1}H 1D nuclear magnetic resonance (NMR) spectra of exemplary samples with the concentration range 1.0 M - 2.0 M DES (pure malicine, malicine + 1 mg/g CAF, malicine + 12.5 mg/g CAF) in D_2O were measured to confirm no occurrence of thermally induced esterification of the carboxylic acid forming the NADES [29]. All NMR measurements were performed at least a week after sample preparation, to verify the stability of the ternary solutions. The selected samples were remeasured one, two, or three weeks after the NMR sample preparation with no observed changes in the obtained results. All samples were stored at RT in a dark place. No precipitation of PC was observed up to a month after the first NMR measurements.

2.4. Mixtures of NADES, H_2O and phenolic compounds

The oversaturated mixtures of NADES, H_2O, and PC were prepared by adding 200 mg of a dry phenolic compound to 2 mL of glyceline- or malicine-based binary solution with 25 wt% H_2O each. Next, the ternary mixtures were stirred for 24 h at 40°C, after which the remaining undissolved phenolic compound was removed by filtration on a mixed cellulose ester syringe filter (0.45 μm), to obtain a clear liquid sample. Samples were diluted 200-fold with acidified milli-q water (2% formic

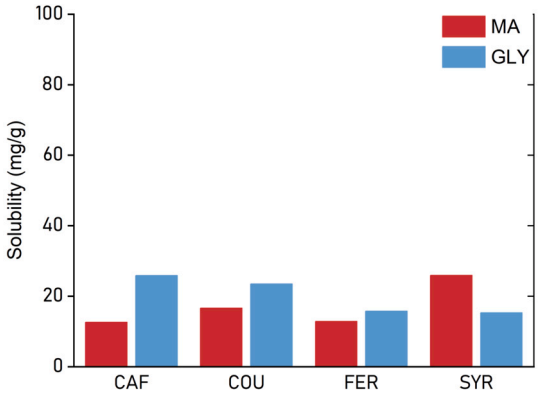

Fig. 3. Solubility of phenolic compounds (PC) in 1:1 ChCl:MA (malicine, red) and 1:2 ChCl:Gly (glyceline, blue) natural deep eutectic solvents (NADES) with 25 wt% H_2O. The bar chart shows the solubility expressed as miligram (mg) of PC per gram of NADES. **CAF:** caffeic acid; **COU:** *p*-coumaric acid; **FER:** ferulic acid; **SYR:** syringaldehyde.

acid). The diluted samples were analyzed using HPLC, and phenolic content was determined based on the external calibration curve, following the protocol in [18].

2.5. NMR measurements

All NMR measurements were performed using a JNMR-ECZ 400 s spectrometer with a magnetic field of 9.4 T, and dedicated Delta V6.1.0 software. The data was further Fourier-transformed, and phase- and baseline-corrected using MestReNova V14.3.2. software. The NMR labeling pattern is presented in Fig. S1.

Samples based on 1:2 ChCl:Gly solvent were transported to 5 mm-diameter NMR tubes flushed with N_2 gas at RT. Samples based on 1:1 ChCl:MA were heated to 80°C using a heating-stirring plate inside of a glovebox, and then transported to 5 mm-diameter NMR tubes. All NMR samples contained deuterated water capillaries for an external lock and reference. The purity of NADES used for sample preparation was confirmed using ^{1}H NMR.

Standard one-dimensional (1D) single-pulse ^{1}H experiments were acquired at RT (1:2 ChCl:Gly DES) or 50°C (1:1 ChCl:MA DES) with an additional 15 min equilibration before the acquisition. ^{1}H-^{1}H Nuclear Overhauser Effect Spectroscopy (NOESY) and ^{1}H-^{1}H Rotating Frame Nuclear Overhauser Effect (ROESY) two-dimensional (2D) experiments were acquired at RT (1:2 ChCl:Gly DES) or 40°C (1:1 ChCl:MA DES) with 15 min equilibration time before acquisition. Both, NOESY and ROESY experiments were performed using at least four different mixing times between 50 ms and 300 ms.

The cross- and diagonal-peak intensities were extracted from the NOESY and ROESY measurements, normalized using Eq. (1) [30], where I_A and I_B are intensities of the diagonal peaks, and I_{AB} and I_{BA} are the intensities of corresponding cross peaks, and used to calculate the cross-relaxation rates and dipolar couplings from the slope of the NOE build-up [31]:

$$I = \frac{I_{AB} \times I_{BA}}{I_A \times I_B}. \quad (1)$$

3. Results and discussion

3.1. Solubility of phenolic compounds in pure NADES

The suitability of NADES as efficient extraction media is frequently linked to the high adaptability of their HB network to the presence of dopants, usually an HBA or secondary HBD [32,33]. Thus, the first step to understanding the role of DES-PC HB formation in ternary solutions is to assess the overall solubility patterns of PC, depending on the chemical structure of both solvent and solute molecules.

As depicted in Fig. 2, pure malicine (red) and glyceline (blue) show high solubility of CAF, COU, FER, and SYR. The polyol-based solvent dissolves between 50 and 75 mg/g of PC, whereas the carboxylic-based solvent reaches a maximum of 25-30 mg/g. The values presented for the latter, although lower in comparison with ChCl:Gly NADES, remain equal or higher than those known for the most commonly used extraction organic solvents, e.g. methanol or ethanol, 10-20 mg/mL for the selected PC [34–36].

Both DES are hydrophilic [37,38], and the presented solubility differs not only between the two solvents but also for the selected PC. First, it could be associated with the significantly increased rigidity of the solvent network in malicine, originating from the selection of a dicarboxylic acid as the HBD, facilitating the dual-site HB network formation [39]. As a consequence, this NADES has 1.5-times higher viscosity ($\eta_{malicine}$ = 446 mPa/s, and $\eta_{glyceline}$ = 309 mPa/s), even if water is added as a secondary HBD [40]. Moreover, the experimental and theoretical studies of malicine have revealed the solvent self-clustering behavior, leading to the formation of ionic domains comparable to those observed in ILs. Adding water and/or quaternary HBD does not disturb the solvent network until relatively large quantities of dopants are reached [41].

In the case of glyceline, a 50% oversaturation of the HBA with HBD in the pure solvent leads to excess OH groups in Gly forming Gly-Gly HBs [42]. This effect is comparable with the self-structuring behavior of the solvent confirmed in the neat glycerol network [43]. Due to lower viscosity, and thus higher mass transfer and overall transport properties [10,44], the overall solvent network in glyceline can adapt to the presence of higher quantities of solute molecules. The excess hydroxyl groups are also available to form HB with the PC, while the solvent network remains preserved.

3.2. Solubility of phenolic compounds in NADES and H_2O mixtures

Glyceline, among polyol-based NADES displays higher extraction yields than other DES [45]. Its superior efficiency to other eutectic solvents is also displayed in Fig. 3, showing solubility of PC in ternary solutions consisting of NADES hydrated with 25 wt% H_2O, confirmed to not disrupt the solvent HB network [31,46]. In malicine-water solutions, the solubilities of all PC are unaffected or decreased by a maximum of 25% when compared to the pure solvent, whereas the solubilities in glyceline decreased by 50 mg/g for CAF and COU, or by 35 mg/g for FER and SYR. This discrepancy is associated with a significant difference in the impact of small quantities of water on the solvent's HB network. The addition of water to malicine has less impact on its physicochemical properties, so the dissolution of PC remains a challenge comparable to that in the neat solvent [39]. The viscosity of carboxylic acid-based NADES formed using solid-state acids is confirmed to remain insensitive to the varying HBA:HBD ratio, the addition of secondary HBD, e.g. water, and mildly responsive to high temperatures [47]. It is confirmed that water molecules do not form HB with HBA or HBD in malicine, but rather aggregate in the existing solvent network. Contrary to that, the addition of water to glyceline is known to improve its overall physicochemical properties [48]. However, this does not imply a direct connection to a better dissolution of PC. Hydration of polyol-based NADES changes the polarity of the solvent and therefore the solubility of PC could decrease compared to pure DES [10,49].

3.3. Solvent network

During the dissolution of PC in glyceline, ^{1}H 1D NMR measurements were performed at RT, at each step of titration to observe changes in the resonances assigned to the hydroxyl groups in HBA and HBD. The formation of HB bonds in NADES eases the chemical exchange of the corresponding labile protons [50]. In the NMR spectra, this is represented with characteristic peak patterns. These can be observed depending on

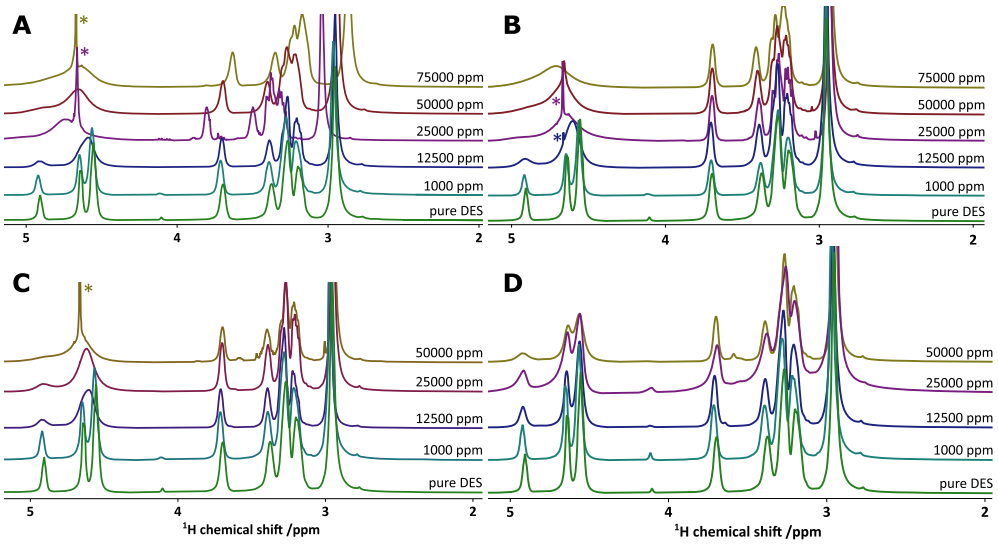

Fig. 4. ^{1}H 1D NMR spectra acquired at RT in 1:2 ChCl:Gly natural deep eutectic solvent (NADES), titrated with four phenolic compounds (PC). **A:** caffeic acid (CAF); **B:** *p*-coumaric acid (COU); **C:** ferulic acid (FER); **D:** syringaldehyde (SYR). The asterisks denote the reference peaks. The assignment of all resonances is available in Fig. S-2.

the timescale of the process. In NADES, a slow proton exchange is expected due to the presence of an extensive HB network that hinders dynamics [51]. In such a scenario, resonances corresponding to all hydroxyl groups (or hydroxyl and carboxyl groups in malicine) participating in the process are well-resolved and easily distinguishable in the ^{1}H NMR spectra, confirming both the close distance between the exchangeable protons and the high rigidity of the solvent network [31].

As presented in Fig. 4 (**A:** CAF; **B:** COU; **C:** FER; and **D:** SYR), the resonances corresponding to the three hydroxyl groups in HBA (deshielded, C3 in Fig. 5; a fully labeled ^{1}H 1D NMR spectrum is available in Fig. S-2) and HBD (shielded, G3 and G4) remain well-resolved in the ^{1}H 1D NMR spectrum of the pure solvent (dark green, bottom). This confirms the rigid arrangement of the solvent network, in which spontaneous proton exchange is expected to occur, however, slowed down to the time scale of NMR acquisition [52].

The addition of small quantities of three hydroxycinnamic acids affects the ^{1}H 1D NMR spectra of glyceline in a similar manner. The changes observed in resonances corresponding to C3, G3, and G4 (Fig. S-1 and S-2) indicate a major rearrangement of the solvent network occurring at 12.5 mg/g of PC. The inner and outer OH groups in the glycerol molecule become more accessible to each other and thus allow unrestricted exchange, frequently associated with the breakdown of the solvent network and loss of eutectic properties. If the NADES are doped with PC and not small molecule dopants, the solvent network becomes more rigid. The large size of the PC molecules has an opposite effect on the solvent network, and decreases instead of increasing the mobility of solvent molecules [32]. These changes, observed in the ^{1}H NMR spectra, are coherent with the results of previous analyses performed on 1:2 and 1:4 ChCl:Gly DES, in which the addition of excess glycerol molecules, without the assigned HBD role in the NADES formation, led to similar NMR observations [31].

In the presence of CAF and COU (Fig. 4A and B, respectively), all OH resonances in Ch^{+} cation and Gly become indistinguishable at 12.5 mg/g, suggesting the unrestricted exchange of protons. On the other hand, the maximum solubility of CAF and COU in the NADES was measured to be 75 mg/g. Thus, the addition of PC causes the rearrangement of glyceline molecules. This can be seen already at low concentrations of the solute, where the PC molecules are located between the aliphatic hydrocarbons. At higher concentrations, the DES network accommodates PC molecules without strongly influencing the hydroxyl groups.

As can be seen in Fig. 4C, the dissolution of FER in glyceline leads to the unrestrained exchange of hydroxyl groups in Ch^{+} only at the maximum PC solubility around 50 mg/g, indicating less impact of the FER molecules accommodated between the aliphatic hydrocarbons in the HBA and HBD. This is despite the fact that FER has a comparable number of OH groups and HBD capacities to COU [53]. Interestingly, no unrestricted proton exchange between the solvent hydroxyl groups is observed in the presence of SYR (Fig. 4D), even at its maximum dissolution. This implies the promotion of HBA-PC and/or HBD-PC interactions that remain below the detection level at low PC concentrations.

The analysis of exchangeable protons dynamics in malicine was not performed due to the presence of the dual-site HBD in the malic acid. This enhances malic acid-malic acid dimeric interactions [39]. Hence, a favorable proton exchange already occurs in the neat solvent (Fig. S2). Moreover, the extreme broadening of resonances due to significantly slower dynamics [54] only allowed the acquisition of qualitative NMR spectra at high temperatures, which are known to influence the proton chemical exchange [47].

3.4. Chemical exchange

Although the concentration of the added PC remains below the detection threshold in the presence of proton-rich solvents, which commonly yields broad and overlapping resonances in liquids with high viscosity [51], their influence on the HB formation between HBA and HBD can still be determined using two-dimensional (2D) NMR spectroscopy. To confirm the molecular arrangement of the selected PC in glyceline solvent network hypothesized based on the ^{1}H 1D NMR spectra, the proton exchange rates (k_{ex} (s^{-1})) were determined using the 2D NOESY and ROESY NMR pulse sequences [55,56].

Due to the systematically progressive peak broadening observed in the ^{1}H 1D spectra, the values of k_{ex} for the hydroxycinnamic acids could only be determined in the presence of 1 mg/g of PC (Fig. 5B), and for all concentrations in the glyceline-SYR ternary solutions (Fig. 5C) [56]. The labeling of the specific proton exchange patterns is presented in Fig. 5A. The exchange rates do not present as absolute values coherent for different samples, hence the different determined k_{ex} are best interpreted on a case-per-case basis. Their relative magnitudes measured within one sample, indicate how certain interactions strengthen or weaken, respectively. Theycan also be further used to estimate the distance between protons [57].

A

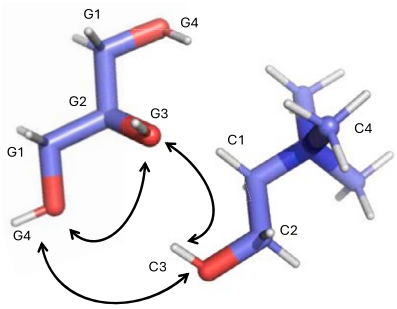

B

	pure	CAF	COU	FER	SYR
C3-G3	0.63 ±0.08	3.05 ±0.21	3.15 ±0.11	2.81 ±0.25	1.19 ±0.22
C3-G4	0.84 ±0.09	3.07 ±0.14	3.08 ±0.03	2.88 ±0.15	1.64 ±0.21
G3-G4	1.20 ±0.09	4.48 ±0.56	2.45 ±0.63	3.18 ±0.69	1.73 ±0.17

C

	pure	1 mg/g	12.5 mg/g	25 mg/g
C3-G3	0.63 ±0.08	1.19 ±0.22	4.09 ±0.97	4.91 ±0.75
C3-G4	0.84 ±0.09	1.64 ±0.21	2.79 ±0.89	4.26 ±0.93
G3-G4	1.20 ±0.09	1.73 ±0.17	2.78 ±0.55	3.33 ±0.50

Fig. 5. A: Schematic representation of the OH-OH exchange rates k_{ex} (s^{-1}) presented in **B** and **C**. **B:** The OH-OH k_{ex} determined for pure 1:2 choline chloride:glycerol (glyceline) natural deep eutectic solvent (NADES) and solutions containing phenolic compounds: caffeic acid (**CAF**); *p*-coumaric acid (**COU**); ferulic acid (**FER**); and syringaldehyde (**SYR**). **C**: The OH-OH k_{ex} determined for pure glyceline NADES and solutions containing 1 mg/g, 12.5 mg/g or 25 mg/g of SYR.

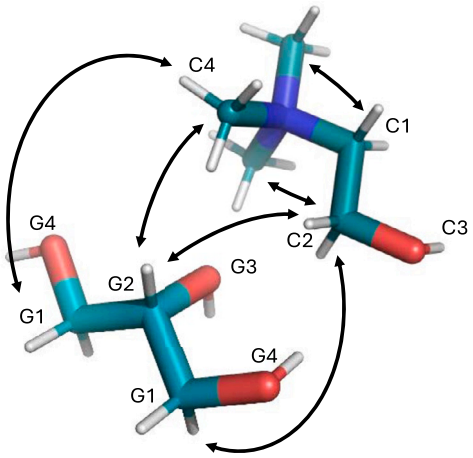

Fig. 6. Dipolar couplings (σ s^{-1}) determined in the solutions of 1:2 ChCl:Gly (glyceline) natural deep eutectic solvent.

The k_{ex} values obtained for pure glyceline suggest the strongest interactions to occur intra- or intermolecularly, between the inner (G3) and outer (G4) OH groups in a glycerol molecule. The Ch^+-Gly interactions seem to be stronger for G4 than for G3, confirming that only part of the hydroxyl groups are present in the solvation of the HBA cation due to its 50% oversaturation with HBD. This confirms that the OH groups in Gly, which do not participate in the solvation of Ch^+, self-cluster (k_{ex} (G3-G4) » k_{ex} (C3-G4)), or solvate the Cl^- anions [58].

In Fig. 5B, differences in k_{ex} (C3-G3) and k_{ex} (C3-G4) are presented for 1 mg/g concentration of all extracts. In the presence of CAF, the magnitude of k_{ex} (G3-G4) and the k_{ex} (Ch^+-G3,G4) interactions remain comparable with the pure solvent. This confirms the negligible influence of CAF-NADES HB formation on the arrangement of the solvent network, previously hypothesized based on ^{1}H 1D NMR in Fig. 4. In the case of COU and FER, all three k_{ex} equilibrate, whereas in the presence of SYR only k_{ex} (C3-G4) equilibrates with k_{ex} (G3-G4). Thus, the Ch^+-inner OH in Gly remains the least preferential interaction in the presence of phenolic formaldehyde.

All four PC achieve comparably high solubilities in glyceline. However, their distribution in the NADES network seems to differ via changes in molecular structure. First, the number and distribution of the hydroxyl and/or carboxyl groups is a known factor contributing to their solubility in HB-based DES networks, because it governs the density of the HB solute-solvent network [53]. The two adjacent hydroxyl groups in the CAF molecule favor the formation of the HB network, observed as a lack of selectivity in k_{ex} values. COU and FER, both sharing a similar structure and one less hydroxyl group than CAF, were previously confirmed to prefer interacting with each other rather than with HBA [32], introducing a steric effect impacting the strength of the HBA-HBD interactions.

SYR, the least substituted PC in this study, is also confirmed to form the lowest number of HB during NADES formation [33]. As presented in Fig. 5C, the addition of 12.5 mg/g and 25 mg/g of SYR to glyceline, changes the molecular arrangement of the solvent. At higher concentrations, k_{ex} (C3-G4) and k_{ex} (G3-G4) become smaller than k_{ex} (C3-G3), implying the distribution of SYR molecules between the aliphatic protons, and consequently, the smaller Ch^+-Gly interactions' contribution to the HB network formation.

3.5. Dipolar couplings

Finally, the magnitude of the ^{1}H-^{1}H dipolar coupling (σ s^{-1}) between the relevant spins (Fig. 6) was determined based on 2D NOESY (Fig. S3) and ROESY NMR experiments [42]. The reciprocal of σ is proportional to the effective distance between the corresponding aliphatic-aliphatic proton interaction. It can become a relevant source of information about the structural arrangement of the NADES molecular network in ternary solutions with high concentrations of PC, in which the exchange resonances are no longer well-resolved.

The values of σ for six pairs of protons were determined in glyceline (Fig. 7A - Fig. 7F) and three pairs in malicine (Fig. 8B - Fig. 8D) at RT and 40°C, respectively. All results were normalized using the value of σ(C1-C2) in Ch^+, assumed to be a stable interaction in the least flexible fragment of the HBA cation [59].

In Fig. 7A, σ(C2-G2) is presented as a function of the wt% of CAF (red), COU (blue), FER (yellow), and SYR (green), and compared with pure glyceline (yellow, additionally labeled with an arrow). At 1 mg/g of extract, no significant difference is seen when compared to the pure solvent, with only mild deviation up to 10%. At 12.5 mg/g and 25 mg/g concentration, σ(C2-G2) in glyceline with CAF, COU, and FER systematically increases, before dropping for all at 50 mg/g and 75 mg/g in the presence of CAF and COU. Thus, the distance between the aliphatic fragments of Ch^+ and Gly returns to its initial stage in pure solvent. This trend remains coherent with the ^{1}H 1D NMR spectra comparison for CAF and COU in Fig. 4A and B. At 50 mg/g, the glyceline-FER solution shows the well-resolved resonance of C3 in Ch^+, but not C3 and C4 in Gly. This implies a smaller sterical disturbance of the HBA cation by the presence of PC. Such a difference can be explained by the additional methoxy group in FER, allowing FER to form intramolecular HB with the neighboring hydroxyl group [60].

σ(C2-G1) in Fig. 7B remains similar for FER and SYR, showing a maximum at 25 mg/g, despite well-resolved 1D ^{1} NMR spectra. Due to the presence of two methoxy groups in the vicinity of the hydroxyl group, SYR can also form intramolecular HB that could hinder its interactions with the neighboring NADES acceptor or donor [61]. On the contrary, the presence of CAF and COU does not disturb the C2-G1 proton pair. A similar effect is seen in Fig. 7C, where all PC have negligible

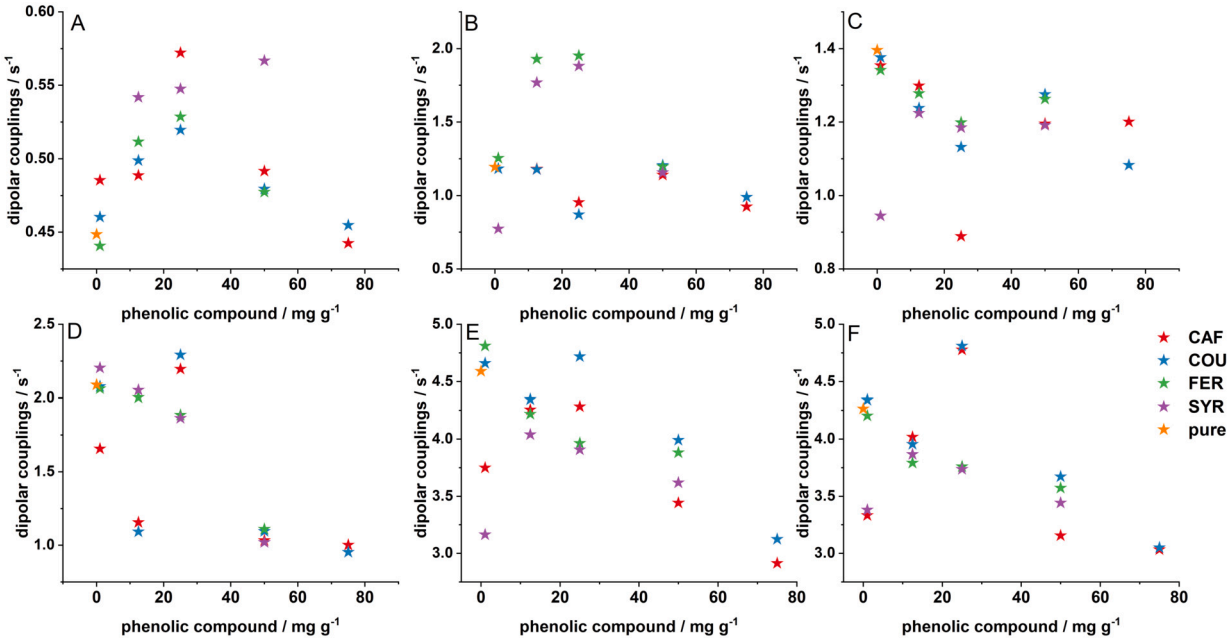

Fig. 7. A: σ(C2-G2) presented as a function of the concentration of PC in mg/g. **B:** σ(C2-G1) presented as a function of the concentration of PC in mg/g. **C:** σ(C2-C4) presented as a function of the concentration of PC in mg/g. **D:** σ(C4-G2) presented as a function of the concentration of PC in mg/g. **E:** σ(C4-G1) presented as a function of the concentration of PC in mg/g. **F:** σ(C4-C1) presented as a function of the concentration of PC in mg/g. **CAF:** caffeic acid (red); **COU:** *p*-coumaric acid (blue); **FER:** ferulic acid (green); **SYR:** syringaldehyde (purple); pure glyceline (yellow).

influence on the magnitude of the intramolecular coupling σ(C2-C4). Fig. 7E-F show the intermolecular interactions of C4 with G2, and G1 and C1, respectively. Similarly to Fig. 7B, the major change for all PC is observed at 25 mg/g. Beyond that, the interactions remain constant, but nearly twice as small. σ(C4-G1) begins to decrease at 25 mg/g, and the intramolecular σ(C4-C1) shows a systematic decrease by 30%.

In malicine, the intermolecular σ(M2-C4) (Fig. 8B) is affected by higher PC concentrations, whereas intermolecular σ(C2-C4) and σ(C1-C4) remain unaffected, with the presence of SYR having the highest constants. Intramolecular values are also smaller for malicine than for glyceline.

In summary, the multi-step NMR analysis of the changes in the HB pattern of NADES in the presence of PC depicts two separate effects governing the solubility of the extract in NADES. First, the basic solubility of 20-30 mg/g of PC in malicine, or in glyceline with added water, is revealed. As can be seen in the ^{1}H 1D NMR spectrum, malicine is a solvent with a rigid HB network, caused by the close vicinity of multiple hydroxyl and carboxyl groups, leading to unrestricted proton chemical exchange slowed down by the network rigidity, however, still too fast to perform chemical exchange analysis, due to the peak broadening. Its HBA-HBD interactions are confirmed to be insensitive to the addition of water. One can thus assume that it will be insensitive to the presence of other HB donors, such as PC. Together with the analysis of dipolar couplings, this confirms the distribution of PC dopants between the aliphatic protons. In glyceline, at low concentrations of PC, the extract molecules are also confirmed to be distributed between aliphatic protons rather than between the hydroxyl groups. This can be confirmed with the σ(C2-G2) and σ(C2-G1) being lower than the analogous σ(C4-G2) and σ(C4-G1). Only in the presence of higher concentrations of CAF and COU, the PC are observed to interact with the hydroxyl groups of Gly and Ch^{+}. The FER and SYR show lower solubility in glyceline due to their ability to form the intramolecular HB between the hydroxyl and neighboring methoxy groups. This effect is more pronounced in SYR, which contains more methoxy groups.

In the presence of 25% water, the solubility of the PC in glyceline decreases to the values observed in malicine, because the OH groups in NADES are engaged in forming HB with water rather than other dopants [38]. The presence of additional OH groups in CAF and COU is no longer improving their solubility. This effect originates from the hydroxyl and carboxyl groups in malicine not participating in the HB formation with PC. Because water molecules are known to have a higher binding affinity to hydroxyl protons in glyceline [31], the solubility of PC observed in the presence of 25 wt% H_2O could be linked to the presence of PC between the aliphatic chains.

4. Summary and conclusions

In this study, the influence of four exemplary PC (CAF, COU, FER and SYR) on the HB network formation of two NADES based on different HBD selection and HBA:HBD molecular ratios were analyzed using 1D and 2D NMR spectroscopy.

Despite significant differences between the physicochemical properties of glyceline (1:2 ChCl:Gly) and malicine (1:1 ChCl:MA), two natural deep eutectic solvents, both can accommodate a comparable number of PC molecules between their aliphatic protons. The presence of hydroxyl groups in the PC structure allows them to yield higher solubility, whereas the presence of methoxy groups attached to a neighboring carbon suppresses this property.

Our results show that although the concentration of added phenolics remains below the detection level in NMR spectroscopy, their impact on the hydrogen bonds forming the solvent network can be analyzed in depth using a systematic analysis of HBA-HBD interactions, leading to important insights into the dissolution mechanism.

CRediT authorship contribution statement

Dries Bleus: Writing – original draft, Visualization, Validation, Methodology, Investigation, Conceptualization. **Renaud B. Jolivet:** Writing – review & editing, Supervision, Resources, Funding acquisition. **Wouter Marchal:** Writing – review & editing, Supervision, Resources, Project administration, Funding acquisition, Conceptualization. **Dries Vandamme:** Writing – review & editing, Supervision, Resources, Project administration, Funding acquisition, Conceptualization. **Katarzyna Dziubinska-Kuehn:** Writing – original draft, Visualization, Project administration, Methodology, Investigation, Conceptualization.

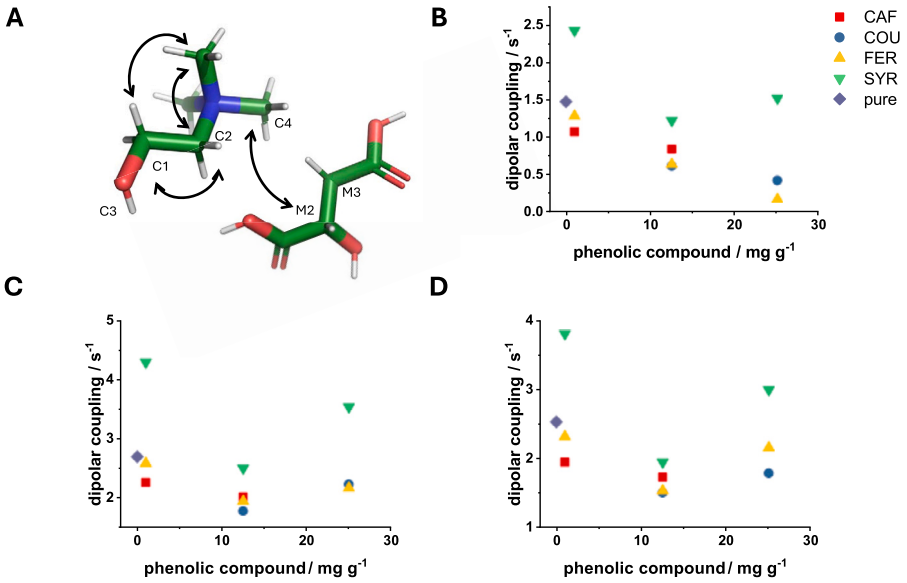

Fig. 8. A: Dipolar couplings (σ s^{-1}) determined in the solutions of 1:1 ChCl:MA (malicine) natural deep eutectic solvent. **B:** σ(M2-C4) presented as a function of the concentration of PC in mg/g. **C:** σ(C2-C4) presented as a function of the concentration of PC in mg/g. **D:** σ(C4-C1) presented as a function of the concentration of PC in mg/g. **CAF:** caffeic acid (red); **COU:** *p*-coumaric acid (blue); **FER:** ferulic acid (yellow); **SYR:** syringaldehyde (green), pure malicine (purple).

Funding

This work was supported by the Bijzonder Onderzoeksfonds BOF (BOF20OWB02) at Hasselt University and the Universiteitsfonds Limburg SWOL (CoBes23.055) at Maastricht University.

Declaration of competing interest

The authors declare that they have no known competing financial interests or personal relationships that could have appeared to influence the work reported in this paper.

Acknowledgements

Authors would like to acknowledge Laura Kollau from Maastricht University for technical support and Philippe De Schryver from Hasselt University for HPLC analysis.

Appendix A. Supplementary material

Supplementary material related to this article can be found online at https://doi.org/10.1016/j.molliq.2025.128147.

Data availability

Data will be made available on request.

References

[1] Sze Ying Lee, João A.P. Coutinho, Melanie Weingarten, Sustainable recovery of microbial-derived natural pigments using deep eutectic solvents: advances, potential, and challenges, Sep. Purif. Technol. 361 (2025) 131413, https://doi.org/10.1016/j.seppur.2025.131413.

[2] Yves Paul Mbous, Maan Hayyan, Adeeb Hayyan, Won Fen Wong, Mohd Ali Hashim, Chung Yeng Looi, Applications of deep eutectic solvents in biotechnology and bioengineering — Promises and challenges, Biotechnol. Adv. 35 (2) (2017) 105–134, https://doi.org/10.1016/j.biotechadv.2016.11.006.

[3] Shiliang Liu, Mingzhe Zhang, Baokun Huang, Nannan Wu, Shunli Ouyang, Raman spectroscopy for the competition of hydrogen bonds in ternary (H_2O-THF-DMSO) aqueous solutions, Molecules 24 (20) (2019), https://doi.org/10.3390/molecules24203666.

[4] Daniela Millán, Cristian Malebran, Rodrigo Ormazábal-Toledo, Towards a rational design of natural deep eutectic solvents for the extraction of polyphenols from Luma apiculata, J. Mol. Liq. 372 (2023) 121155, https://doi.org/10.1016/j.molliq.2022.121155.

[5] Jie Cheng, Yuxin Qiu, Jiahui Chen, Yuqi Gu, Jingwen Wang, Guzhong Chen, Zhiwen Qi, Zhen Song, Rational design and experimental evaluation of novel amino acid-based natural deep eutectic solvents for CO_2 capture, Sep. Purif. Technol. 361 (2025) 131554, https://doi.org/10.1016/j.seppur.2025.131554.

[6] Dariane Trivisiol da Silva, Roberson Pauletto, Sabrina da Silva Cavalheiro, Vivian Caetano Bochi, Eliseu Rodrigues, Julia Weber, Cristiane de Bona da Silva, Fernando Dal Pont Morisso, Milene Teixeira Barcia, Tatiana Emanuelli, Natural deep eutectic solvents as a biocompatible tool for the extraction of blueberry anthocyanins, J. Food Compos. Anal. 89 (2020) 103470, https://doi.org/10.1016/j.jfca.2020.103470.

[7] Andrew P. Abbott, Glen Capper, David L. Davies, Raymond K. Rasheed, Vasuki Tambyrajah, Novel solvent properties of choline chloride/urea mixtures, Chem. Commun. 1 (2003) 70–71, https://doi.org/10.1039/b210714g.

[8] Andrew P. Abbott, Glen Capper, David L. Davies, Helen L. Munro, Raymond K. Rasheed, Vasuki Tambyrajah, Preparation of novel, moisture-stable, Lewis-acidic ionic liquids containing quaternary ammonium salts with functional side chains, Chem. Commun. 1 (19) (2001) 2010–2011, https://doi.org/10.1039/b106357j.

[9] Magdalena Espino, María de los Ángeles Fernández, Federico J.V. Gomez, María Fernanda Silva, Natural designer solvents for greening analytical chemistry, TrAC, Trends Anal. Chem. 76 (2016) 126–136, https://doi.org/10.1016/j.trac.2015.11.006.

[10] Yuntao Dai, Geert Jan Witkamp, Robert Verpoorte, Young Hae Choi, Tailoring properties of natural deep eutectic solvents with water to facilitate their applications, Food Chem. 187 (2015) 14–19, https://doi.org/10.1016/j.foodchem.2015.03.123.

[11] Rubén F. González-Laredo, Víctor Iván Sayago-Monreal, Martha Rocío Moreno-Jiménez, Nuria Elizabeth Rocha-Guzmán, José Alberto Gallegos-Infante, Luisa Fernanda Landeros-Macías, Martha Rosales-Castro, Natural deep eutectic solvents (NaDES) as an emerging technology for the valorisation of natural products and agro-food residues: a review, Int. J. Food Sci. Technol. 58 (12) (2023) 6660–6673, https://doi.org/10.1111/ijfs.16641.

[12] Sanja Milošević, Anica Bebek Markovinović, Nemanja Teslić, Aleksandra Mišan, Milica Pojić, Irena Brčić Karačonji, Karlo Jurica, Dario Lasić, Predrag Putnik, Danijela Bursać Kovačević, Branimir Pavlić, Use of natural deep eutectic solvent (NADES) as a green extraction of antioxidant polyphenols from strawberry tree fruit (Arbutus unedo L.): an optimization study, Microchem. J. 200 (2024) 110284, https://doi.org/10.1016/j.microc.2024.110284.

[13] Tongnian Gu, Mingliang Zhang, Ting Tan, Jia Chen, Zhan Li, Qinghua Zhang, Hongdeng Qiu, Deep eutectic solvents as novel extraction media for phenolic compounds from model oil, Chem. Commun. 50 (2014) 11749–11752, https://doi.org/10.1039/C4CC04661G.

[14] Noorfatimah Yahaya, Ahmad Husaini Mohamed, Muhammad Sajid, Nur Nadhirah, Mohamad Zain, Pao-Chi Liao, Kit Wayne Chew, Deep eutectic solvents as sustainable extraction media for extraction of polysaccharides from natural sources: status, challenges and prospects, Carbohydr. Polym. 338 (2024) 122199, https://doi.org/10.1016/j.carbpol.2024.122199.

[15] Negar Nooraee Nia, Mohammad Reza Hadjmohammadi, Amino acids- based hydrophobic natural deep eutectic solvents as a green acceptor phase in two-phase hollow fiber-liquid microextraction for the determination of caffeic acid in coffee, green tea, and tomato samples, Microchem. J. 164 (2021) 106021, https://doi.org/10.1016/j.microc.2021.106021.

[16] Tomislav Bosiljkov, Filip Dujmić, Marina Cvjetko Bubalo, Janez Hribar, Rajko Vidrih, Mladen Brnčić, Emil Zlatic, Ivana Radojčić Redovniković, Stela Jokić, Natural deep eutectic solvents and ultrasound-assisted extraction: Green approaches for extraction of wine lees anthocyanins, Food Bioprod. Process. 102 (2017) 195–203, https://doi.org/10.1016/j.fbp.2016.12.005.

[17] Baranse Ozturk, Charles Parkinson, Maria Gonzalez-Miquel, Extraction of polyphenolic antioxidants from orange peel waste using deep eutectic solvents, Sep. Purif. Technol. 206 (2018) 1–13, https://doi.org/10.1016/j.seppur.2018.05.052.

[18] Dries Bleus, Heike Blockx, Emma Gesquiere, Peter Adriaensens, Pieter Samyn, Wouter Marchal, Dries Vandamme, High-temperature hydrothermal extraction of phenolic compounds from Brewer's spent grain and malt dust biomass using natural deep eutectic solvents, Molecules 29 (9) (2024) 1983, https://doi.org/10.3390/molecules29091983.

[19] Juan C. López-Linares, Víctor Campillo, Mónica Coca, Susana Lucas, María T. García-Cubero, Microwave-assisted deep eutectic solvent extraction of phenolic compounds from Brewer's spent grain, J. Chem. Technol. Biotechnol. 96 (2) (2021) 481–490, https://doi.org/10.1002/jctb.6565.

[20] Sofia Chanioti, Maria Katsouli, Constantina Tzia, Novel processes for the extraction of phenolic compounds from olive pomace and their protection by encapsulation, Molecules 26 (6) (2021), https://doi.org/10.3390/molecules26061781.

[21] Paula Virginia de Almeida Pontes, Isabella Ayumi Shiwaku, Guilherme José Maximo, Eduardo Augusto Caldas Batista, Choline chloride-based deep eutectic solvents as potential solvent for extraction of phenolic compounds from olive leaves: extraction optimization and solvent characterization, Food Chem. 352 (2021) 129346, https://doi.org/10.1016/j.foodchem.2021.129346.

[22] Zannou Oscar, Ilkay Koca, Greener extraction of anthocyanins and antioxidant activity from blackberry (Rubus spp) using natural deep eutectic solvents, LWT 158 (2022) 113184, https://doi.org/10.1016/j.lwt.2022.113184.

[23] Yubing Yang, Mengdi Guan, Mengdan Fang, Ying Gu, Lunzhao Yi, Dabing Ren, Simultaneous extraction and selective separation of catechins, caffeine and theanine from waste tea residue facilitated by citric acid-based deep eutectic solvent, Sep. Purif. Technol. 360 (2025) 130918, https://doi.org/10.1016/j.seppur.2024.130918.

[24] Derong Lin, Mengshi Xiao, Jingjing Zhao, Zhuohao Li, Baoshan Xing, Xindan Li, Maozhu Kong, Liangyu Li, Qing Zhang, Yaowen Liu, Hong Chen, Wen Qin, Hejun Wu, Saiyan Chen, An overview of plant phenolic compounds and their importance in human nutrition and management of type 2 diabetes, Molecules 21 (10) (2016), https://doi.org/10.3390/molecules21101374.

[25] Naresh Kumar, Nidhi Goel, Phenolic acids: natural versatile molecules with promising therapeutic applications, Biotechnol. Rep. 24 (2019) e00370, https://doi.org/10.1016/j.btre.2019.e00370.

[26] Zeb Alam, Concept, mechanism, and applications of phenolic antioxidants in foods, J. Food Biochem. 44 (9) (2020) e13394, https://doi.org/10.1111/jfbc.13394.

[27] J.E. O'Connell, P.F. Fox, Significance and applications of phenolic compounds in the production and quality of milk and dairy products: a review, Int. Dairy J. 11 (3) (2001) 103–120, https://doi.org/10.1016/S0958-6946(01)00033-4.

[28] Kyung Hwa Hong, Phenol compounds treated cotton and wool fabrics for developing multi-functional clothing materials, Fiber Polym. 16 (2015) 565–571, https://doi.org/10.1007/s12221-015-0565-0.

[29] Nerea Rodriguez Rodriguez, Adriaan van den Bruinhorst, Laura J.B.M. Kollau, Maaike C. Kroon, Koen Binnemans, Degradation of deep-eutectic solvents based on choline chloride and carboxylic acids, ACS Sustain. Chem. Eng. 7 (13) (2019) 11521–11528, https://doi.org/10.1021/acssuschemeng.9b01378.

[30] Lianne H.E. Wieske, Máté Erdélyi, Non-uniform sampling for NOESY? A case study on spiramycin, Magn. Reson. Chem. 59 (7) (2021) 723–737, https://doi.org/10.1002/mrc.5133.

[31] Katarzyna Dziubinska-Kühn, Marion Pupier, Jörg Matysik, Jasmine Viger-Gravel, Beatrice Karg, Magdalena Kowalska, Time-dependent hydrogen bond network formation in glycerol-based deep eutectic solvents, ChemPhysChem 23 (10) (2022) e202100806, https://doi.org/10.1002/cphc.202100806.

[32] Shan Yuhang, Han Yingyi, Fan Chen, Liu Yang, Xueli Cao, New natural deep eutectic solvents based on aromatic organic acids, Green Chem. Lett. Rev. 14 (4) (2021) 713–719, https://doi.org/10.1080/17518253.2021.2009579.

[33] Jiae Ryu, Mairui Zhang, Yunxuan Wang, Ruoqian Li, Kwang Ho Kim, Arthur J. Ragauskas, Gyu Leem, Min Bum Park, Chang Geun Yoo, Impacts of hydrogen bond donor structures in phenolic aldehyde deep eutectic solvents on pretreatment efficiency, Energy Fuels 38 (17) (2024) 16441–16450, https://doi.org/10.1021/acs.energyfuels.4c02301.

[34] Wenqin Ji, Qingqing Meng, Lei Ding, Fang Wang, Jiejie Dong, Guangyi Zhou, Baohua Wang, Measurement and correlation of the solubility of caffeic acid in eight mono and water+ethanol mixed solvents at temperatures from (293.15 to 333.15) K, J. Mol. Liq. 224 (2016) 1275–1281, https://doi.org/10.1016/j.molliq.2016.10.110.

[35] Meilia Yoseba Tarigan, Mehrdad Ebrahimi, Separation and purification of vanillin and syringaldehyde from an oxidized kraft liquor – A mini review, Chem. Ing. Tech. 96 (4) (2024) 418–431, https://doi.org/10.1002/cite.202300224.

[36] Alexander Kaufmann, Lukas Maier, Marlene Kienberger, Solvent screening for the extraction of aromatic aldehydes, Sep. Purif. Technol. 340 (2024) 126780, https://doi.org/10.1016/j.seppur.2024.126780.

[37] Víctor Hernández-Serrano, José Muñoz-Embid, Fernando Bergua, Carlos Lafuente, Manuela Artal, pVT behaviour of hydrophilic and hydrophobic eutectic solvents, J. Mol. Liq. 382 (2023) 122019, https://doi.org/10.1016/j.molliq.2023.122019.

[38] Oliver Hammond, Ria Atri, Daniel Bowron, Karen Edler, Neutron diffraction study of indole solvation in deep eutectic systems of choline chloride, malic acid, and water, Chemistry 28 (2022) e202200566, https://doi.org/10.1002/chem.202200566.

[39] Oliver S. Hammond, Daniel T. Bowron, Andrew J. Jackson, Thomas Arnold, Adrian Sanchez-Fernandez, Nikolaos Tsapatsaris, Victoria Garcia Sakai, Karen J. Edler, Resilience of malic acid natural deep eutectic solvent nanostructure to solidification and hydration, J. Phys. Chem. B 121 (31) (2017) 7473–7483, https://doi.org/10.1021/acs.jpcb.7b05454.

[40] Jennifer Osamede Airouyuwa, Hussein Mostafa, Asad Riaz, Sajid Maqsood, Utilization of natural deep eutectic solvents and ultrasound-assisted extraction as green extraction technique for the recovery of bioactive compounds from date palm (Phoenix dactylifera L.) seeds: an investigation into optimization of process parameters, Ultrason. Sonochem. 91 (2022) 106233.

[41] Yilin Xie, Herui Liu, Li Lin, Maojun Zhao, Li Zhang, Yunsong Zhang, Yichao Wu, Application of natural deep eutectic solvents to extract ferulic acid from Ligusticum chuanxiong Hort with microwave assistance, RSC Adv. 9 (2019) 22677–22684, https://doi.org/10.1016/j.ultsonch.2022.106233.

[42] Carla C. Fraenza, Ramez A. Elgammal, Mounesha N. Garaga, Sahana Bhattacharyya, Thomas A. Zawodzinski, Steven G. Greenbaum, Dynamics of glyceline and interactions of constituents: a multitechnique NMR study, J. Phys. Chem. B 126 (4) (2022) 890–905, https://doi.org/10.1021/acs.jpcb.1c09227.

[43] Ying Liu, Kama Huang, Yanping Zhou, Dezhi Gou, Hongxiao Shi, Hydrogen bonding and the structural properties of glycerol–water mixtures with a microwave field: a molecular dynamics study, J. Phys. Chem. B 125 (29) (2021) 8099–8106, https://doi.org/10.1021/acs.jpcb.1c03232.

[44] Carmine D'Agostino, Lynn F. Gladden, Mick D. Mantle, Andrew P. Abbott, Essa I. Ahmed, Azhar Y.M. Al-Murshedi, Robert C. Harris, Molecular and ionic diffusion in aqueous-deep eutectic solvent mixtures: probing inter-molecular interactions using PFG NMR, Phys. Chem. Chem. Phys. 17 (23) (2015) 15297–15304, https://doi.org/10.1039/C5CP01493J.

[45] Ashish Pandey, Rewa Rai, Mahi Pal, Siddharth Pandey, How polar are choline chloride-based deep eutectic solvents?, Phys. Chem. Chem. Phys. 16 (4) (2014) 1559–1568, https://doi.org/10.1039/C3CP53456A.

[46] M.J. Roldán-Ruiz, R.J. Jiménez-Riobóo, M.C. Gutiérrez, M.L. Ferrer, F. del Monte, Brillouin and NMR spectroscopic studies of aqueous dilutions of malicine: determining the dilution range for transition from a "water-in-DES" system to a "DES-in-water" one, J. Mol. Liq. 284 (2019) 175–181, https://doi.org/10.1016/j.molliq.2019.03.133.

[47] Jennifer Osamede Airouyuwa, Hussein Mostafa, Meththa Ranasinghe, Sajid Maqsood, Influence of physicochemical properties of carboxylic acid-based natural deep eutectic solvents (CA-NADES) on extraction and stability of bioactive compounds from date (Phoenix dactylifera L.) seeds: an innovative and sustainable extraction technique, J. Mol. Liq. 388 (2023) 122767, https://doi.org/10.1016/j.molliq.2023.122767.

[48] Yuntao Dai, Jaap van Spronsen, Geert-Jan Witkamp, Robert Verpoorte, Young Hae Choi, Natural deep eutectic solvents as new potential media for green technology, Anal. Chim. Acta 766 (2013) 61–68, https://doi.org/10.1016/j.aca.2012.12.019.

[49] Júlia B. Barbieri, Caroline Goltz, Flávia Batistão Cavalheiro, Aline Theodoro Toci, Luciana Igarashi-Mafra, Marcos R. Mafra, Deep eutectic solvents applied in the extraction and stabilization of rosemary (Rosmarinus officinalis L.) phenolic compounds, Ind. Crop. Prod. 144 (2020) 112049, https://doi.org/10.1016/j.indcrop.2019.112049.

[50] Alex D. Bain, Chemical exchange in NMR, Prog. Nucl. Magn. Reson. Spectrosc. 43 (3) (2003) 63–103, https://doi.org/10.1016/j.pnmrs.2003.08.001.

[51] Ignacio Delso, Carlos Lafuente, José Muñoz-Embid, Manuela Artal, NMR study of choline chloride-based deep eutectic solvents, J. Mol. Liq. 290 (2019) 111236, https://doi.org/10.1016/j.molliq.2019.111236.

[52] Ryan Stefanovic, Michael Ludwig, Grant B. Webber, Rob Atkin, Alister J. Page, Nanostructure, hydrogen bonding and rheology in choline chloride deep eutectic solvents as a function of the hydrogen bond donor, Phys. Chem. Chem. Phys. 19 (2017) 3297–3306, https://doi.org/10.1039/C6CP07932F.

[53] Nikolaos Prinos, Maria Myrto Dardavila, Epaminondas Voutsas, Measurement and thermodynamic modelling of the solubilities of caffeic acid, p-coumaric acid and ferulic acid in three choline chloride-based deep eutectic solvents, J. Chem. Thermodyn. 197 (2024) 107335, https://doi.org/10.1016/j.jct.2024.107335.

[54] Srijan Chatterjee, Tubai Chowdhury, Sayan Bagchi, Solvation dynamics and microheterogeneity in deep eutectic solvents, J. Phys. Chem. B 128 (51) (2024) 12669–12684, https://doi.org/10.1021/acs.jpcb.4c06295.

[55] Rudolph Willem, 2D NMR applied to dynamic stereochemical problems, Prog. Nucl. Magn. Reson. Spectrosc. 20 (1) (1988) 1–94, https://doi.org/10.1016/0079-6565(88)80008-6.

[56] Gizem Oruc, Tereza Varnali, Somer Bekiroglu, Hydroxy protons as structural probes to reveal hydrogen bonding properties of polyols in aqueous solution by NMR spectroscopy, J. Mol. Struct. 1160 (2018) 319–327, https://doi.org/10.1016/j.molstruc.2018.02.017.

[57] Ryszard Michalczyk, Irina M. Russu, Determination of distances involving exchangeable protons from NOESY spectra of two DNA dodecamers, FEBS Lett. 331 (3) (1993) 217–222, https://doi.org/10.1016/0014-5793(93)80340-z.
[58] Yannik Hinz, Joachim Beerwerth, Roland Böhmer, Anion dynamics and motional decoupling in a glycerol–choline chloride deep eutectic solvent studied by one- and two-dimensional 35Cl NMR, Phys. Chem. Chem. Phys. 25 (2023) 28130–28140, https://doi.org/10.1039/d3cp03668e.
[59] Joachim Seelig, Hans-Ulrich Gally, Roland Wohlgemuth, Orientation and flexibility of the choline head group in phosphatidylcholine bilayers, Biochim. Biophys. Acta, Biomembr. 467 (2) (1977) 109–119, https://doi.org/10.1016/0005-2736(77)90188-2.
[60] Sosthene Nyomba Kamanda, Ayesha Jacobs, Multicomponent crystals of p-coumaric acid and trans-ferulic acid: structures and physicochemical properties, J. Mol. Struct. 1244 (2021) 130830, https://doi.org/10.1016/j.molstruc.2021.130830.
[61] Tsonko Kolev, Rüdiger Wortmann, Michael Spiteller, William S. Sheldrick, Maik Heller, 4-hydro-xy-3, 5-di-methoxy-benz-aldehyde (syring-aldehyde), Acta Crystallogr., Sect. E 60 (8) (2004) o1387–o1388, https://doi.org/10.1107/S1600536804017015.